

Solving the multiple peeling and discovering a new angle for the optimal nanoadhesion of insects, spiders and geckos

Nicola M. Pugno¹, Stanislav N. Gorb²

¹*Department of Structural Engineering,*

Politecnico di Torino, Torino, Italy; nicola.pugno@polito.it

²*Department of Functional Morphology and Biomechanics, Zoological Institute of the University of Kiel, Germany; sgorb@zoologie.uni-kiel.de*

Keywords: multiple peeling, nano, adhesion, insects, spiders, geckos

SUMMARY. Herewith we solve the multiple peeling problem by applying a fracture mechanics approach to a complex system of films, adhering to the substrate and having a common hinge, where the pulling force is applied. The system consisting of two peeling tapes is considered as a case study. The main result of our theoretical considerations is that an optimal peeling angle, at which adhesion is maximal, does exist. The solution is validated in experiments using polymeric adhesive tapes. These results aid to explain the functional mechanism of biological adhesive systems of insects, spiders, and geckos bearing tape-like spatula-shaped contact elements.

1. INTRODUCTION

The capacity of geckos and other animals to adhere to inverted surfaces is well known [2-5]. The functional mechanism of adhesion is related to the presence of hierarchical, from the nano- to macro-scale geometry of their feet [6-10]. For example, in Tokay gecko, the adhesive system consists of hierarchical structures ranging from macroscopic lamellae (flexible tape-like structures, 1000 μm long) covered by setae (30-130 μm long and 5-10 μm in diameter) to setal branches called spatulae (0.1-0.2 μm wide and 0.015-0.020 μm thick) responsible for contact formation with the substrate. Recently, numerous studies [11-22] have discussed factors allowing the gecko to adhere and detach from surfaces. Van der Waals attraction [21] and wetting phenomena [22] have been demonstrated to be key mechanisms involved in the gecko adhesion.

Similar to geckos, many other animals, such as beetles, flies and spiders, possess the ability to move on vertical surfaces and ceilings [23, 24]. This ability arises from the micro/nanostructures of their attachment pads. It is noteworthy that with an increase of the animal mass, the size of the terminal attachment elements decreases and their density increases [15]. Insects terminal elements are covered with the fluid, whereas spiders and geckos exhibit the most versatile and effective dry adhesion known in nature. Mimicking such biological adhesive systems for technological applications could lead to a revolution in materials science of adhesives [25-28].

Since insects, spiders and geckos possess spatula-like terminal contact elements on the tips of their adhesive setae, the Kendall model [29], describing mechanical behaviour of the single peeling tape, can be applied to explain adhesion control by varying the peeling angle. Even if the peeling geometry is appropriate to describe behaviour of the single spatula, simultaneous peeling of many

spatulae, having different orientation in the opposite digits and contralateral legs, and thus a more complex architecture, must be considered to describe forces generated by living animals. Here we have solved the multiple peeling problem and found out an optimal angle for maximum adhesion for this kind of contact geometry. The solution is validated in experiments using polymeric adhesive tapes. These results aided in explanation of the functional mechanism of biological adhesive systems of insects, spiders, and geckos bearing tape-like spatula-shaped contact elements, Figure 0.

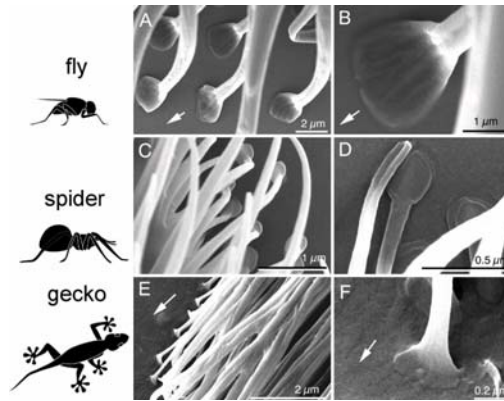


Figure 0. Example of terminal contact units: a 2D adhesive tape like geometry emerges.

2. MULTIPLE PEELING

Let us consider a three-dimensional complex system composed by N adhesive tapes converging to a common point P , where an external force \vec{F} is applied. Each tape has cross-section area A_i , Young modulus Y_i , length l_i and orientation defined by the unitary vector \vec{n}_i , see Figure 1.

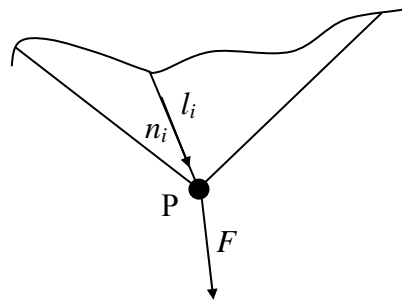


Figure 1. Diagram of the multiple peeling system considered in this study (eq. 1).

The elastic displacement $\delta\bar{\eta}$ (assumed to be small, i.e. tape orientations do not change significantly) of the point P can be calculated as follows. The elongation of each tape is $\delta l_i = \delta\bar{\eta} \times \bar{n}_i$, thus the tape tension (if negative, the corresponding tape does not work, and the external load is supported by the other tapes) is $\bar{T}_i = \delta l_i \bar{n}_i Y_i A_i / l_i = k_i \delta\bar{\eta} \times \bar{n}_i \bar{n}_i$, where $k_i = Y_i A_i / l_i$ is the tape stiffness. The equilibrium of the material point (hinge) P, where the load is applied, imposes $\sum_{i=1}^N \bar{T}_i = \bar{F}$ or equivalently $[K] \delta\bar{\eta} = \bar{F}$, where $[K]$ is the known (by comparing the last two equations) stiffness matrix of the system. The elastic displacement $\delta\bar{\eta}$ is thus calculated as:

$$\delta\bar{\eta} = [K]^{-1} \bar{F} \quad (1a)$$

from which the tape elongations δl_i , tensions T_i and strains ε_i can be evaluated:

$$\delta l_i = \delta\bar{\eta} \times \bar{n}_i, T_i = k_i \delta l_i, \varepsilon_i = \delta l_i / l_i, \quad i=1, \dots, N \quad (1b)$$

Imagine to impose a finite (the tape orientations change significantly) displacement $\Delta\bar{\eta}$ at the point P, to be accommodated by multiple *virtual* delaminations Δl_i and elastic elongations of the tapes. A new global configuration, denoted by the symbol prime, takes place, see Figure 2. From the scheme reported in Fig. 2 we deduce the validity of the following equations:

$$\bar{l}_i (1 + \varepsilon_i) + \Delta \bar{l}_i + \Delta \bar{\eta} = \bar{l}'_i (1 + \varepsilon'_i), \quad \bar{l}_i = l_i \bar{n}_i, \bar{l}'_i = (l_i + \Delta l_i) \bar{n}'_i, \quad i=1, \dots, N \quad (2)$$

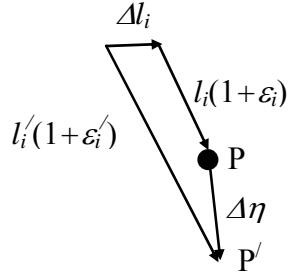


Figure 2. Finite delamination of the i th tape (eq. 2).

The strains ε_i are known and their current values ε_i' can be derived, according to eq. (1), as a function of the unknown orientations \bar{n}_i' . Accordingly, coupling eqs. (1b) and (2), we can write $4N$ scalar equations in $4N$ unknowns: the N amplitudes of the virtual delaminations Δl_i (their directions are known *a priori* from the configuration of adhering tapes), the N current strains ε_i' and the $2N$ significant components of the new tape orientations \bar{n}_i' ($n_i' = 1$).

Inverting the previous problem, assuming as known three delamination amplitudes in eq. (2), we could derive the other compatible delaminations as well the displacement $\Delta \bar{\eta}$ of the point P. This means that only three virtual delaminations can be considered as independent.

The virtual forces F_i required for the delamination of the i^{th} tape can be calculated by the Griffith's energy balance. Accordingly, the delamination takes place when:

$$-\partial \Pi / \partial l_i = 2\gamma_i w_i, \quad \Pi = E - W, \quad i=1, \dots, N \quad (3a)$$

where Π is the total potential energy, E is the elastic energy, W is the external work, γ_i is the surface energy of the i^{th} tape/substrate interface and w_i is its width.

The elastic energy variation can be calculated as:

$$\Delta E = \frac{1}{2} \sum_{i=1}^N A_i l_i Y_i (\varepsilon_i'^2 - \varepsilon_i^2) \quad (3b)$$

The variation of the external work is:

$$\Delta W = \bar{F} \times \Delta \bar{\eta} \quad (3c)$$

The real critical force is:

$$F_c = \min\{F_i\} = F_j \quad (3d)$$

and corresponds to the delamination of the j^{th} tape.

The algebraic system is nonlinear but can be linearized considering the differentials instead of the finite differences (e.g. $\Delta \bar{\eta} \rightarrow d\bar{\eta}$). However note that the physical system remains intrinsically geometrically nonlinear due to the existence of the orientation variations. Moreover, the energy balance remains non linear in the force F .

3. DOUBLE PEELING

The developed treatment is here applied to study a double peeling system, Figure 3. From eq. (1) we derive:

$$T_1 = F \frac{\sin(\theta + \alpha_2)}{\sin(\alpha_1 + \alpha_2)}, \quad T_2 = F \frac{\sin(\theta - \alpha_1)}{\sin(\alpha_1 + \alpha_2)}, \quad \varepsilon_i = T_i / (Y_i A_i)$$

The previous equations are valid for $T_{1,2} > 0$ thus for $\alpha_1 < \theta < \pi - \alpha_2$. If a tension is negative only the other tape sustains the entire load and thus we have a classical single peeling (if both the tensions are negative the load cannot be in equilibrium).

From eq. (2) we have:

$$\left\{ \begin{array}{l} l_1(1 + \varepsilon_1)\cos\alpha_1 + \Delta l_1 + \Delta u = (l_1 + \Delta l_1)(1 + \varepsilon'_1)\cos(\alpha_1 + \Delta\alpha_1) \\ l_1(1 + \varepsilon_1)\sin\alpha_1 + \Delta v = (l_1 + \Delta l_1)(1 + \varepsilon'_1)\sin(\alpha_1 + \Delta\alpha_1) \\ l_2(1 + \varepsilon_2)\cos\alpha_2 + \Delta l_2 - \Delta u = (l_2 + \Delta l_2)(1 + \varepsilon'_2)\cos(\alpha_2 + \Delta\alpha_2) \\ l_2(1 + \varepsilon_2)\sin\alpha_2 + \Delta v = (l_2 + \Delta l_2)(1 + \varepsilon'_2)\sin(\alpha_2 + \Delta\alpha_2) \\ \varepsilon'_1 = \frac{F}{Y_1 A_1} \frac{\sin(\theta + \alpha_2 + \Delta\alpha_2)}{\sin(\alpha_1 + \alpha_2 + \Delta\alpha_2 + \Delta\alpha_1)} \\ \varepsilon'_2 = \frac{F}{Y_2 A_2} \frac{\sin(\theta - \alpha_1 - \Delta\alpha_1)}{\sin(\alpha_1 + \alpha_2 + \Delta\alpha_2 + \Delta\alpha_1)} \end{array} \right.$$

where Δu and Δv are the horizontal and vertical components of the displacement $\Delta \bar{\eta}$. Note that the classical single peeling only requires one equation, since no angle and strain variations occur during delamination.

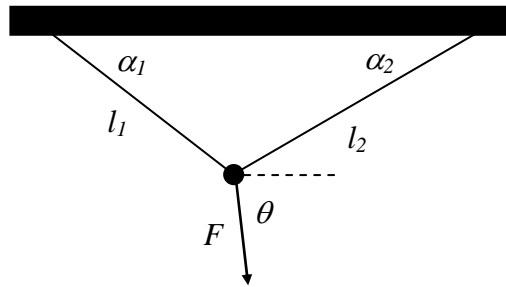


Figure 3. Diagram of the double peeling system considered.

Considering $\Delta \varepsilon_i = \varepsilon_i' - \varepsilon_i$ and solving the previous system in the limit of small variations (i.e. substituting the finite differences with the differentials), yields:

$$[A] = \begin{bmatrix} 1 & 0 & l_1(1+\varepsilon_1)\sin\alpha_1 & 0 & -l_1\cos\alpha_1 & 0 \\ 0 & 1 & -l_1(1+\varepsilon_1)\cos\alpha_1 & 0 & -l_1\sin\alpha_1 & 0 \\ -1 & 0 & 0 & l_2(1+\varepsilon_2)\sin\alpha_2 & 0 & -l_2\cos\alpha_2 \\ 0 & 1 & 0 & -l_2(1+\varepsilon_2)\cos\alpha_2 & 0 & -l_2\sin\alpha_2 \\ 0 & 0 & \sin(\theta+\alpha_2)\cos(\alpha_1+\alpha_2) & \sin(\theta-\alpha_1) & \sin^2(\alpha_1+\alpha_2)Y_1A_1/F & 0 \\ 0 & 0 & \sin(\theta+\alpha_2) & \sin(\theta-\alpha_1)\cos(\alpha_1+\alpha_2) & 0 & \sin^2(\alpha_1+\alpha_2)Y_2A_2/F \end{bmatrix}$$

$$[b_1] = \begin{bmatrix} (1+\varepsilon_1)\cos\alpha_1 - 1 \\ (1+\varepsilon_1)\sin\alpha_1 \\ 0 \\ 0 \\ 0 \\ 0 \end{bmatrix}, \quad [b_2] = \begin{bmatrix} 0 \\ 0 \\ (1+\varepsilon_2)\cos\alpha_2 - 1 \\ (1+\varepsilon_2)\sin\alpha_2 \\ 0 \\ 0 \end{bmatrix}, \quad [dx] = \begin{bmatrix} du \\ dv \\ d\alpha_1 \\ d\alpha_2 \\ d\varepsilon_1 \\ d\varepsilon_2 \end{bmatrix}$$

$$[dx] = [A]^{-1}([b_1]dl_1 + [b_2]dl_2)$$

Eq. (3b) in the limit of small variations, gives:

$$dE = Y_1A_1l_1\varepsilon_1d\varepsilon_1 + Y_2A_2l_2\varepsilon_2d\varepsilon_2 + \frac{1}{2}Y_1A_1\varepsilon_1^2dl_1 + \frac{1}{2}Y_2A_2\varepsilon_2^2dl_2$$

as well as eq. (3c) poses:

$$dW = F \cos \theta du + F \sin \theta dv$$

According to eq. (3a) and (3d) the delamination force can now be easily obtained.

For example, considering the symmetric case ($\alpha_1 = \alpha_2 = \alpha$, $l_1 = l_2 = l$, $\theta = \pi/2$, and consequently $u = 0$ and $\varepsilon_1 = \varepsilon_2 = \varepsilon$) we find the following solutions:

$$d\varepsilon = \frac{1 - (1 + \varepsilon)\cos\alpha}{\frac{1 + \varepsilon}{\varepsilon} \frac{\sin^2\alpha}{\cos\alpha} + \cos\alpha} \frac{dl}{l} \cong \frac{(1 - \cos\alpha)\cos\alpha}{\sin^2\alpha} \varepsilon \frac{dl}{l}$$

$$d\alpha = \frac{[(1 + \varepsilon)\cos \alpha - 1]dl + l \cos \alpha d\varepsilon}{l(1 + \varepsilon)\sin \alpha} \cong \frac{\cos \alpha - 1 + \varepsilon + l \cos \alpha d\varepsilon/dl}{\sin \alpha} \frac{dl}{l}$$

$$dv = l(1 + \varepsilon)\cos \alpha d\alpha + l \sin \alpha d\varepsilon + (1 + \varepsilon)\sin \alpha dl$$

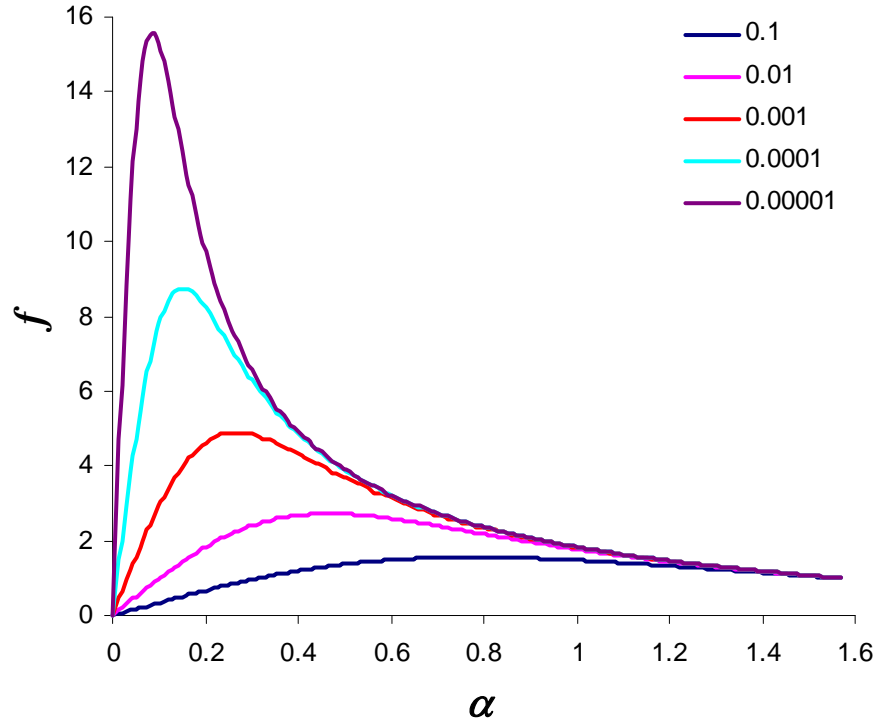


Figure 4. Dimensionless force $f = F_c(\alpha)/F_c(\alpha = \pi/2)$ versus angle α by varying the dimensionless adhesion strength λ ; $F_c(\alpha = \pi/2) = 2YA(-1 + \sqrt{1 + 4\lambda})$: a new angle for optima adhesion emerges.

The previous equations have been linearized in ε . Accordingly, the energy balance is self-consistently written considering terms up to the second power of ε . The result yields:

$$\varepsilon^2 + 2(1 - \cos \alpha)\varepsilon - 4\lambda = 0,$$

where $\lambda = \frac{\gamma}{tY}$ and $t = A/w$ is the tape thickness. Solving this equation, the critical value of the strain ε_C for delamination is obtained. The previous equation is surprising: it is identical to that of the single peeling problem. However the force required for delamination is different since here we have:

$$F_C = 2YA\varepsilon_C \sin \alpha$$

thus only for $\alpha = \pi/2$ the prediction is that of the single peeling tape loaded by a force $F/2$, for which $F_C = 2YA\varepsilon_C$, as it must physically be.

The delamination force is thus:

$$F_C = 2YA \sin \alpha \left(\cos \alpha - 1 + \sqrt{(1 - \cos \alpha)^2 + 4\lambda} \right)$$

The behaviour is depicted in Figure 4. An angle for optimal adhesion α_{opt} clearly emerges as a function of the parameter λ .

4. EXPERIMENTS ON ADHESIVE TAPES AND INSECTS

It is plausible to assume that biological adhesive systems try to actively use changes in the geometry of their adhesive system to maximize adhesion by keeping peeling geometry close to the optimal angle and to minimize adhesion by increasing the angle by digit hyperextension. In insects, spiders, and geckoes, there are several hierarchical levels of structures responsible for maintaining of an optimal peeling angle and for switching the system to the non-adhesive state.

In order to prove this assumption and above theoretical considerations, we have carried out an experiment with double peeling system made of rigid and flexible adhesive tape.

Adhesive rubber tapes connected through the hinge were loaded with different mass at two distinct initial peeling angles. After the system came to the equilibrium, the final peeling angle at the equilibrium was recorded (Figure 5, inset). The results clearly demonstrate the presence of the optimal peeling angle. For given rubber elasticity and adhesive energy, the optimal angle was approximately at 65° (Figure 5). In the case of the rigid adhesive tape, the optimal angle was not detected: the highest mass was kept at the shallowest angle (0°).

Preliminary experiments on beetle *Chrysolina fastuosa*, Figure 6, suggest the importance of considering the multiple peeling and the existence of an optimal angle for maximal adhesion (work in progress).

Obtained theoretical and experimental results support our initial idea that for elastic tapes an optimum peeling angle does exist. This result is of a great importance for the explanation of the functional mechanism of biological adhesives and for adhesive technology as well.

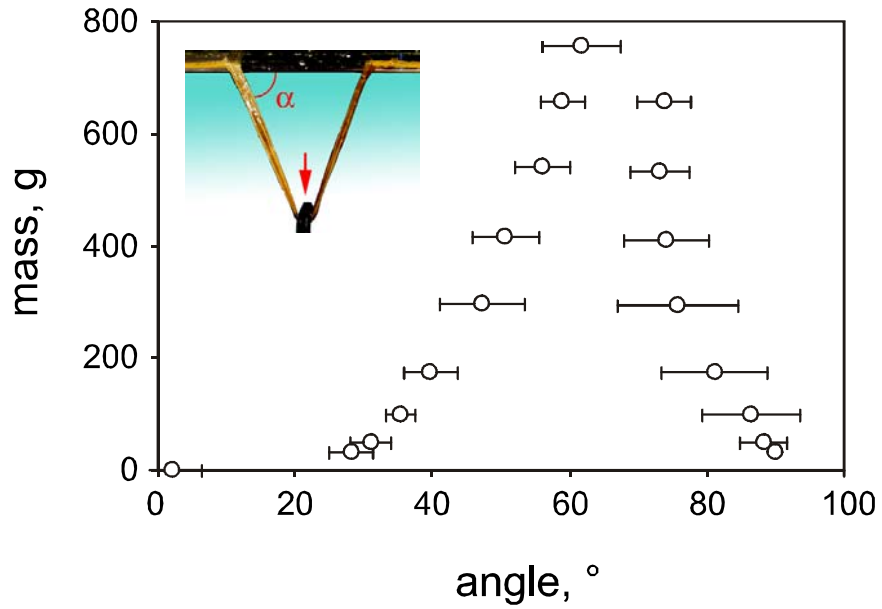


Figure 5. Equilibrium peeling condition for elastic adhesive rubber: the predicted new angle for optimal adhesion is confirmed.

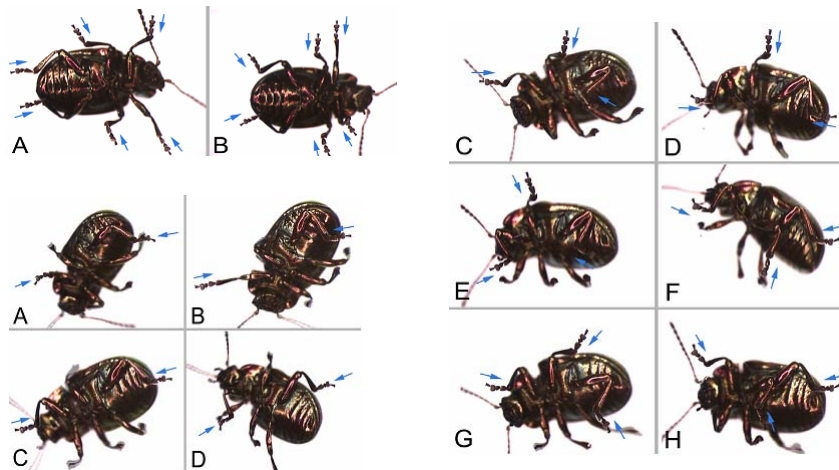


Figure 6. Six, three and two legged beetle *Chrysolina fastuosa* on a ceiling suggest the importance of considering a multiple peeling approach, the animal changes its adhesion angle according to theory (work in progress).

5. CONCLUSION

Herewith we have solved the multiple peeling problem. The system consisting of two peeling tapes is considered as a case study. The main result of our theoretical considerations is that an optimal peeling angle, at which adhesion is maximal, does exist. This result is of a great importance for the explanation of the functional mechanism of biological adhesives and for adhesive technology as well.

REFERENCES

- [1] Aristotle, *Historia Animalium*, 343 B.C. See Book IX, Part 9, translated by Thompson DAW, http://classics.mit.edu/Aristotle/history_anim.html.
- [2] Simmermacher, G., *Zeitschr Wiss Zool* **40**, 481-556 (1884).
- [3] Schmidt, H.R., *Jena Z Naturwiss* **39**, 551 (1904).
- [4] Dellit, W. D., *Jena. Z Naturwiss* **68**, 613-658 (1934).
- [5] Ruibal, R. and Ernst, V., *J Morph* **117**, 271-294 (1965).
- [7] Russell, A. P., *J Zool Lond* **176**, 437-476 (1975).
- [8] Russell, A.P., *Can J Zool* **64**, 948-955 (1986).
- [9] Schleich, H. H. and Kästle, W., *Amphib Reptil* **7**, 141-166 (1986).
- [10] Gennaro, J.G.J., *Nat Hist* **78**, 36-43 (1969).
- [11] Hiller, U., *Z Morphol Tiere* **62**, 307-362 (1968).
- [12] Autumn, K., and Peattie, A., *Int Comp Bio* **42**, 1081-1090 (2002)..
- [13] Autumn, K., *MRS Bulletin* **32**, 473-478 (2007)..
- [14] Autumn, K. and Gravish, N., *Philosophical Transactions of the Royal Society of London, Series A: Mathematical, Physical, and Engineering Sciences* **366**, 1575-1590 (2008).
- [15] Arzt, E., Gorb, S., Spolenak, R., *Proc Natl Acad Sci USA* **100**, 10603-10606 (2003).
- [16] Autumn, K. and Peattie, A. M., *Integr Comp Biol* **42**, 1081-1090 (2002).
- [17] Bergmann, P. J., Irschick, D. J., *J Exp Zool* **303A**, 785-791 (2005).
- [18] Huber, G., Gorb, S.N., Spolenak, R. and Arzt, E., *Biol Lett* **1**, 2-4 (2005).
- [19] Autumn, K., Dittmore, A., Santos, D., Spenko, M. and Cutkosky, M., *J. Exp Biol* **209**, 3569-3579 (2006).
- [20] Autumn, K., Hsieh, S. T., Dudek, D. M., Chen, J., Chitaphan, C. and Full, R. J. *J Exp Biol* **209**, 260-272, 2007.
- [21] Autumn, K., Liang, Y. A., Hsieh, S. T., Zesch, W., Chan, W. P., Kenny, T. W., Fearing, R. and Full, R.J., *Nature* **405**, 681-685 (2000).
- [22] Huber, G., Mantz, H., Spolenak, R., Mecke, K., Jacobs, K., Gorb, S. N. and Arzt, E., *Proc Natl Acad Sci USA* **102**, 16293-16296 (2005).
- [23] Stork, N.E., *J Exp Biol* **88**, 91-107 (1980).
- [24] Dai, Z., Gorb, S. N. and Schwarz, U., *J Exp Biol* **205**, 2479-2488 (2002).
- [25] Yurdumakan, B., Raravikar, N. R., Ajayanm P. M. and Dhinojwala, A., *Chem Commun* 3799-3801 (2005).
- [26] Haeshin, L., Bruce, P. L., and Phillip, B. M., *Nature* **448**, 338-341 (2007).
- [27] Pugno, N. M., *J. Phys.: Condens. Matter* **19**, 395001 (17pp) (2007).
- [28] Pugno, N. M., *Nano Today* **3**, 36-42 (2008).
- [29] Kendall, K. *J. Phys. D: Appl. Phys.* **8**, 1449-1452 (1975)